

Spatial distribution on high-order-harmonic generation of an H_2^+ molecule in intense laser fieldsJun Zhang, Xin-Lei Ge, Tian Wang, Tong-Tong Xu, Jing Guo,^{*} and Xue-Shen Liu[†]*Institute of Atomic and Molecular Physics, Jilin University, Changchun 130012, People's Republic of China*

(Received 5 February 2015; published 22 July 2015)

High-order-harmonic generation (HHG) for the H_2^+ molecule in a 3-fs, 800-nm few-cycle Gaussian laser pulse combined with a static field is investigated by solving the one-dimensional electronic and one-dimensional nuclear time-dependent Schrödinger equation within the non-Born-Oppenheimer approximation. The spatial distribution in HHG is demonstrated and the results present the recombination process of the electron with the two nuclei, respectively. The spatial distribution of the HHG spectra shows that there is little possibility of the recombination of the electron with the nuclei around the origin $z = 0$ a.u. and equilibrium internuclear positions $z = \pm 1.3$ a.u. This characteristic is irrelevant to laser parameters and is only attributed to the molecular structure. Furthermore, we investigate the time-dependent electron-nuclear wave packet and ionization probability to further explain the underlying physical mechanism.

DOI: [10.1103/PhysRevA.92.013418](https://doi.org/10.1103/PhysRevA.92.013418)

PACS number(s): 32.80.Rm, 42.50.Hz, 42.65.Ky

I. INTRODUCTION

High-order-harmonic generation (HHG) via laser-matter interaction has been intensively studied in recent years because of its applications in generating isolated attosecond pulses [1–3]. The attosecond pulses are significant for probing, for example, nuclear dynamics and photoelectron wave packets [4,5]. To further describe the HHG process of the H_2^+ molecule, the semiclassical three-step model was presented [6–8]. First, the electron is ionized from the molecule through a tunneling, multiphoton, or over-the-barrier process in the laser field. Second, the electron is accelerated by the laser field and obtains additional kinetic energy. In this process the electron moves only under the effect of a laser field. Finally, when the laser field changes its direction, the electron can recombine not only with its parent nucleus but also with another nucleus [9], which is different from the case of an atom, and is accompanied by the emission of the high-energy photons.

Since the molecular structure is more complex and the degrees of freedom in molecules are more than that in atoms, the harmonic generation of the molecules has been increasingly studied both experimentally and theoretically [10–13]. Except for the motion of the nuclei, the charge-resonance-enhanced ionization [14–16] is also qualitatively different from the atomic case. Guan *et al.* [17] reported the resonance effects in two-photon double-ionization processes of H_2 by femtosecond XUV laser pulses in the fixed-nuclei approximation. Doblhoff-Dier *et al.* [18] simulated the ionization of H_2^+ by comparing the angular distribution of the electron momentum spectra at different laser intensities and internuclear distances.

Most theoretical studies of molecular high-order-harmonic generation (MHOHG) have been restricted to the Born-Oppenheimer approximation [19]. Lein *et al.* [20] investigated the orientation dependence of high-order-harmonic generation at an internuclear distance of $R = 2$ a.u. They also showed that the H_2^+ molecule may give opposite contributions for various electronic positions, so the interference phenomenon exists in HHG, resulting in the suppression of the harmonic emission.

Bian and Bandrauk [21] considered resonant excitation under laser-induced electron transfer and studied the multichannel molecular harmonic generation for asymmetric HeH^{2+} in few-cycle laser pulses; their results showed that the harmonic spectra cutoff has been extended. Bian and Bandrauk [22] also indicated that the phase control also plays an important role in multichannel MHOHG.

There has been much effort to break through the Born-Oppenheimer approximation limitation and take nuclear motion into account. Chelkowski *et al.* [23] investigated dissociative ionization of the one-dimensional (1D) H_2^+ molecular with moving nuclei by projecting onto asymptotic Volkov states and obtained a great deal of information about electron-nuclear dynamics. Bandrauk *et al.* [24] studied the effect of nuclear motion on MHOHG and found that it limits MHOHG efficiency to only few first cycles. Recently, Ge *et al.* [25] investigated the HHG and isolated-attosecond-pulse generation of the H_2^+ molecule by solving the non-Born-Oppenheimer time-dependent Schrödinger equation (TDSE). The numerical results indicate that the nuclear motion leads to an overall weaker harmonic signal as compared to the static case, but the harmonic spectrum is smoother with fewer modulations. Miao and Zhang [26] presented the effects of the nuclear motion on asymmetric molecular harmonic emission from HeH^{2+} and manipulated the recombination channels originating from the nucleus, producing a 48-as pulse.

In this paper we study the HHG process of the H_2^+ molecule through the combination of a Gaussian laser field and a static field by solving the non-Born-Oppenheimer TDSE. We explain the recombination of the electron with the two nuclei in terms of the spatial distribution in HHG. We show that there is little possibility of the recombination of the electron with the nuclei around the origin $z = 0$ a.u. and equilibrium internuclear positions $z = \pm 1.3$ a.u. Furthermore, we also present the time-dependent electron-nuclear wave packet as well as the combined energy of the Coulomb potential and laser field potential to explain the spatial distribution in HHG.

II. THEORETICAL MODEL AND NUMERICAL METHOD

The generation of high-order harmonics can be investigated by means of numerical solution of the non-Born-Oppenheimer

^{*}gjing@jlu.edu.cn[†]liuxs@jlu.edu.cn

TDSE of the H_2^+ molecule. The initial wave function is obtained by diagonalizing the field-free Hamiltonian under a sine discrete variable representation [27] and the ground-state energy is -21.2 eV. In the dipole approximation and the length gauge, the TDSE reads [28] (atomic units are used throughout, unless otherwise stated)

$$i \frac{\partial}{\partial t} \Psi(z, R, t) = H(z, R, t) \Psi(z, R, t) \\ = [T + V_C(z, R) + V_I(z, t)] \Psi(z, R, t), \quad (1)$$

where

$$T = T_R + T_e = -\frac{1}{m_p} \frac{\partial^2}{\partial R^2} - \frac{2m_p + m_e}{4m_p m_e} \frac{\partial^2}{\partial z^2}, \\ V_C(z, R) = \frac{1}{R} - \frac{1}{\sqrt{(z - R/2)^2 + 1}} - \frac{1}{\sqrt{(z + R/2)^2 + 1}}, \\ V_I(z, t) = \left(1 + \frac{m_e}{2m_p + m_e}\right) z E(t).$$

Here T stands for the total kinetic energy of the H_2^+ molecule, which includes the kinetic energy of the nuclei T_R and the electron T_e ; V_C is the soft-core Coulomb potential; V_I is the interaction between the laser and the H_2^+ molecule; R is the internuclear distance (the equilibrium internuclear distance $R = 2.6$ a.u.); and z is the electronic coordinate (with respect to the center of mass of the two nuclei). The z axis is taken to be along the internuclear axis of diatomic molecules. The polarization of the laser pulse is assumed to be parallel to the z axis. The m_e and m_p are the electron and proton masses ($m_e = 1$ a.u. and $m_p = 1836$ a.u.), respectively. The time-dependent wave functions are obtained by using the second-order split-operator approach [29]. The calculations have been performed using the attosecond resolution quantum dynamics program LZH-DICP [30–32].

The ionization probability of electron can be calculated by the flux operator

$$P(t) = \int_0^t dt' \int_0^{R_s} dR j(z, R, t'), \quad (2)$$

where

$$j = \frac{1}{\mu_e} \text{Im} \left(\Psi^* \delta(z - z_0) \frac{\partial}{\partial z} \Psi \right). \quad (3)$$

We use the grid defined by $0 < R < 30$ a.u. and $-100 < z < 100$ a.u., with the spatial steps $\Delta R = 0.1$ a.u. and $\Delta z = 0.2$ a.u., and the time step for the electron is 0.2 a.u. Here $z_0 = 25$ a.u. is the position for flux analysis in the ionization process and $R_s = 25$ a.u. is the absorbing position [26,31,33]. The $\mu_e = \frac{2m_p m_e}{2m_p + m_e}$ is the reduced mass of the electron.

The time evolution of nuclear wave packet distributions can be calculated by

$$P_R(R, t) = \int_{-\infty}^{\infty} dz |\Psi(z, R, t)|^2. \quad (4)$$

The time evolution of electron wave packet distributions can be calculated by

$$P_z(z, t) = \int_0^R dR |\Psi(z, R, t)|^2. \quad (5)$$

According to the Ehrenfest theorem [21,34], the dipole acceleration can be written as

$$a(t) = \frac{d^2}{dt^2} \langle \Psi(z, R, t) | z | \Psi(z, R, t) \rangle \\ = -\langle \Psi(z, R, t) | \frac{dV_C(z, R)}{dz} \\ + \left(1 + \frac{m_e}{2m_p + m_e}\right) E(t) | \Psi(z, R, t) \rangle. \quad (6)$$

The HHG spectrum can be obtained by means of Fourier transformation of the dipole acceleration and the harmonic spectrum is proportional to the modulus squared of the Fourier transform of $a(t)$,

$$P_A(\omega) \sim \left| \frac{1}{T} \int_0^T a(t) e^{-i\omega t} dt \right|^2. \quad (7)$$

If the dipole acceleration is separated into two parts [$a(t) = a(z > 0, t) + a(z < 0, t)$] according to the electronic coordinate, the contributions of the two nuclei to the harmonic generation in the H_2^+ molecule can be investigated via separating the dipole acceleration into two parts $a(z > 0, t)$ and $a(z < 0, t)$ [35,36]. In this work we investigate the spatial distribution on HHG of the H_2^+ molecule in an intense laser field, thus the dipole acceleration distribution in each electronic coordinate can be written as [20]

$$d_A(z, t) = -\int_0^R \Psi^*(z, R, t) \left[\frac{dV_C(z, R)}{dz} \right. \\ \left. + \left(1 + \frac{m_e}{2m_p + m_e}\right) E(t) \right] \Psi(z, R, t) dR. \quad (8)$$

By using the dipole acceleration distribution in each electronic coordinate, the contribution of each electronic coordinate in HHG can be demonstrated.

III. RESULTS AND DISCUSSION

We investigate the HHG process of the H_2^+ molecule generated in the combination of a linearly polarized laser field with a Gaussian envelope and a static laser field

$$E(t) = E_0 f(t) \sin(\omega t) - \alpha E_0, \quad (9)$$

where $f(t) = \exp[-4 \ln 2 (t^2/\tau^2)]$, E_0 is the peak amplitude of the laser field, ω is the frequency, τ is full width at half maximum (FWHM), and α is the static parameter. Figure 1(a1) shows the electric field (blue solid line) and the ionization probability (red dashed line) in a Gaussian laser pulse with the peak intensity $I_1 = 4 \times 10^{14}$ W/cm² and $\alpha = 0$. There are two main peaks marked as P_1 and P_2 , respectively. The ionization probability demonstrates that the H_2^+ molecule begins to ionize around the negative peak P_1 (located at -0.23 o.c.). Accordingly, the time interval between ionization and recombination is about 0.5 o.c. [6,36] and the electron recombines with the nuclei around 0.27 o.c. This is in agreement with the ionization probability, which remains almost unchanged in the region of time from 0.08 to 0.28 o.c. After the laser field reaches its positive peak P_2 , the electron is ionized again and then recombines with the nuclei. To further understand the physical mechanism of the HHG process, we

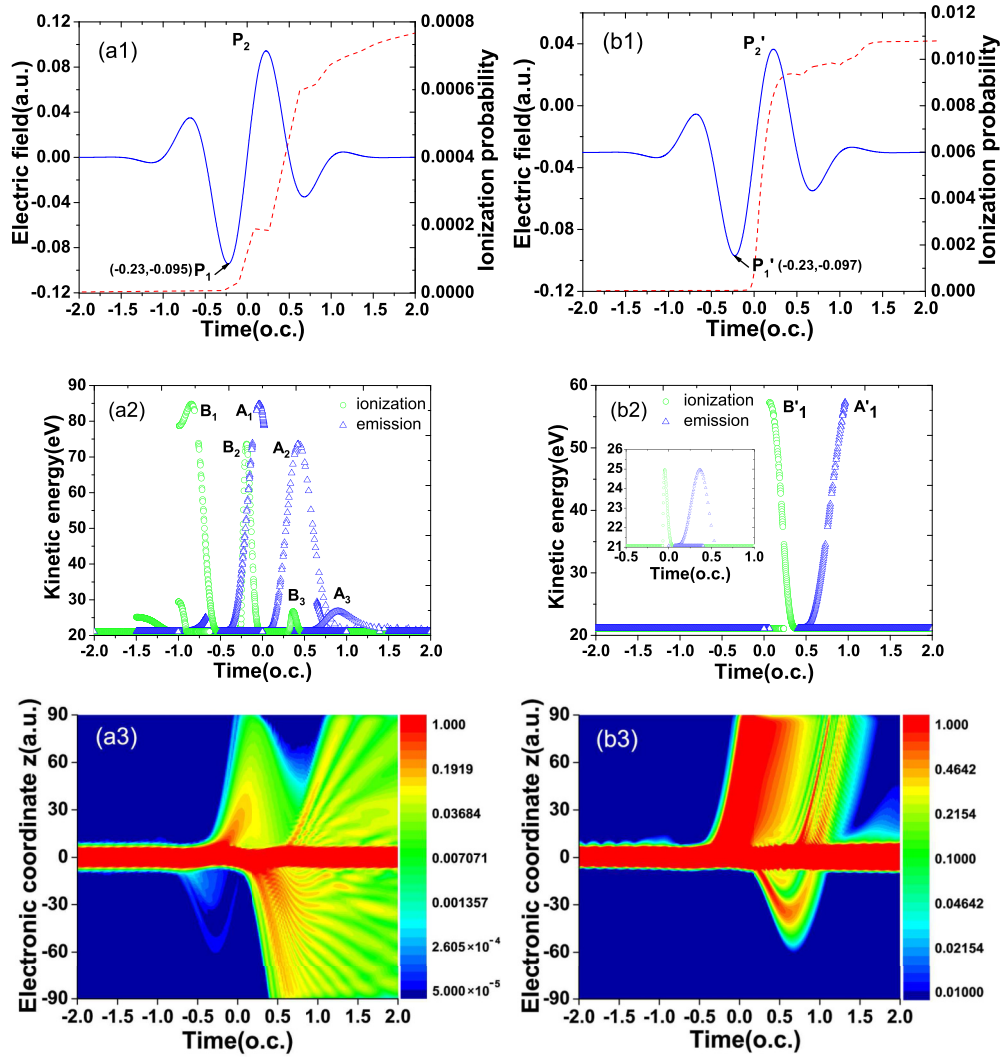


FIG. 1. (Color online) (a1) and (b1) Electric field (blue solid line) and ionization probability (red dashed line) in a Gaussian laser pulse ($\alpha = 0$) and the combination of a Gaussian laser pulse and a static laser field ($\alpha = 0.4$), respectively. (a2) and (b2) Dependence of the harmonic order on the ionization time (green circles) and emission time (blue triangles) in a Gaussian laser pulse ($\alpha = 0$) (the recombination with the nuclei along both the positive- and negative- z directions is shown) and the combination of a Gaussian laser pulse and a static laser field ($\alpha = 0.4$) (only the recombination with the nucleus along the negative- z direction is shown), respectively. The inset in (b2) shows the dependence of the harmonic order on the ionization time (green circles) and emission time (blue triangles) in the region of time from -0.5 to 1.0 optical cycle (o.c.), where only the recombination with the nucleus along the positive- z direction is shown. (a3) and (b3) Electronic probability density $P_z(z, t)$ from -2 to 2 o.c. in a Gaussian laser pulse ($\alpha = 0$) and the combination of a Gaussian laser pulse and a static laser field ($\alpha = 0.4$), respectively.

illustrate the semiclassical electron trajectories in the HHG. Figure 1(a2) shows the dependence of the harmonic order ω/ω_0 on the ionization (green circles) and emission times (blue triangles) in the Gaussian laser pulse ($\alpha = 0$); here the recombination with both nuclei is shown. We consider that the range of the internuclear distance is approximately from $R = 2.6$ to 3.0 a.u. (3.0 a.u. is the maximum internuclear distance obtained from the time evolution of the nuclear probability distribution; we have calculated it, but it is not presented in this paper). Therefore, we assume that the ionized electron has recombined with the nuclei if the electronic coordinate $|z|$ is in the region of 1.3 – 1.5 a.u. Based on this, we try to gradually narrow down the range of the electronic coordinate and find that the illustration shown in Fig. 1(a2) is

almost unchanged. From Fig. 1(a2) one can see that there are three main peaks contributing to the HHG, marked as A_1 , A_2 , and A_3 , respectively. The increase of ionization probability before -0.23 o.c. is very slow [see the red dashed line in Fig. 1(a1)], thus the ionization around the peak B_1 can be ignored, which means that the harmonic emission around peak A_1 can be ignored and only peaks A_2 and A_3 make contributions to the HHG.

Figure 1(a3) shows the time evolution of the electronic probability density from -2 to 2 o.c. The probability of the ionized electron (around $t = -0.75$ o.c.) along the negative- z direction is weak, which is in agreement with the ionization probability in Fig. 1(a1). Figure 1(a3) also shows that the ionized electron (around $t = -0.23$ o.c.) along the positive- z

direction can return to the core and mainly recombine (around $t = 0.27$ o.c.) with the nucleus along the positive- z direction (in our coordinate system). In addition, the ionized electron (around $t = 0.27$ o.c.) along the negative- z direction can also return to the core and mainly recombine (around $t = 0.75$ o.c.) with the nucleus along the negative- z direction (in our coordinate system). Both of these recombination processes make contributions to the high-order-harmonic generation.

To investigate the spatial distribution in HHG and demonstrate the probability of the electron recombined with the nuclei, we could try to just decrease the positive peak intensity while keeping the negative peak intensity unchanged by adding a static laser field on a Gaussian laser field as shown in Fig. 1(b1). Figure 1(b1) shows the electric field (blue solid line) and the ionization probability (red dashed line) in the combination of a linearly polarized laser field with a Gaussian envelope and a static laser field with the peak intensity $I_2 = 2 \times 10^{14}$ W/cm² and $\alpha = 0.4$. Figure 1(b1) indicates that there are two main peaks marked as P'_1 and P'_2 . The ionization probability demonstrates that the H_2^+ molecule begins to ionize around the laser peak P'_1 (located at -0.23 o.c.) and then the ionization probability increases rapidly. In order to describe the role of two nuclei of the H_2^+ molecule in the HHG process, the recombinations with the nucleus along the positive- and negative- z directions are shown, respectively. Figure 1(b2) shows the dependence of the harmonic order ω/ω_0 on the ionization (green circles) and emission times (blue triangles) in the combination of a Gaussian laser pulse and a static laser field ($\alpha = 0.4$); here only the recombination with the nucleus along the negative- z direction is shown. We assume that the ionized electron has recombined with the nuclei if the electronic coordinate $|z|$ is in the region of 1.3–1.5 a.u. Based on this, we try to gradually narrow down the range of the electronic coordinate and find that the illustration shown in Fig. 1(b2) is almost unchanged. The ionization time around the peak B'_1 is greater than 0 o.c. and the corresponding emission time is around the peak A'_1 . The inset in Fig. 1(b2) shows the dependence of the harmonic order on the ionization (green circles) and emission (blue triangles) times, where the ionization time is less than 0 o.c. and only the electronic recombination with the

nucleus along the positive- z direction is shown. Figure 1(b3) shows that the ionized electron (around $t = -0.23$ o.c.) along the positive- z direction cannot return to the core, because the positive laser peak intensity around the peak P'_2 is weak enough. In contrast, the ionized electron (around $t = 0.06$ o.c.) along the negative- z direction can return to the core and mainly recombine with the nucleus along the negative- z direction (in our coordinate system). Explicitly, from Fig. 1(b3) we can see that the recombination process begins at about 0.5 o.c. and ends at about 1.0 o.c. At the beginning the recombination probability is very low, while most of the electrons recombine with the core around 0.75 o.c., which corresponds to the peak A'_1 in Fig. 1(b2), and there is only once recombination in the process. Thus, the electron mainly ionized from -0.23 to 0 o.c. (less than 0 o.c.) in Fig. 1(b2) cannot recombine with the nucleus. Further, the harmonic emission is mainly from the electron recombining with the nucleus along the negative- z direction (in our coordinate system), which is in agreement with Fig. 1(b3).

Figure 2(a) shows the map of the value of $d_A(z, t)$ and its projection to the bottom for the 1D H_2^+ molecule in the Gaussian laser field ($\alpha = 0$) and the expression of $d_A(z, t)$ can be found in Eq. (8). We can see that the value of $d_A(z, t)$ is mainly distributed around the electronic coordinates $z = \pm 2$ and ± 0.75 a.u. In addition, we can clearly see that the absolute value of $d_A(z, t)$ is very small around the origin $z = 0$ a.u. and the equilibrium internuclear positions $z = \pm 1.3$ a.u. To better explain this physical mechanism we demonstrate the spatial distribution in the HHG spectra of the H_2^+ molecule in the Gaussian laser field ($\alpha = 0$) in Fig. 2(b), in which the horizontal axis represents the harmonic order, the vertical axis represents the electronic coordinate, and the depth of the color represents the intensity of the harmonics. Figure 2(b) shows that there is little contribution to the HHG around the origin $z = 0$ a.u. and the equilibrium internuclear positions $z = \pm 1.3$ a.u., which is in agreement with the small absolute value of $d_A(z, t)$ shown in Fig. 2(a). It should be mentioned that it is impossible for the two nuclei to overlap at the origin for the 1D H_2^+ molecule, thus the electron cannot recombine with the nuclei around the origin $z = 0$ a.u., which makes little contribution to the HHG. The electron of the H_2^+ molecule also cannot recombine with the nuclei when it is located within

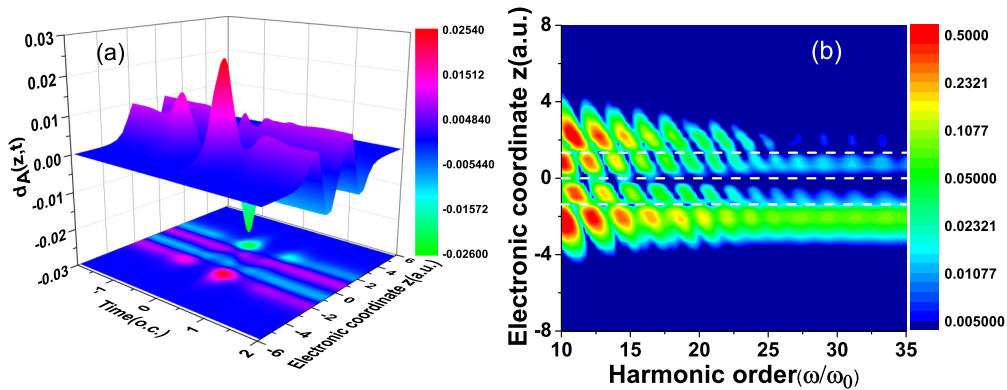


FIG. 2. (Color online) (a) Map of the value of $d_A(z, t)$ and (b) spatial distribution of the HHG spectra as a function of the electronic coordinate and harmonic order for the 1D H_2^+ molecule in the Gaussian laser field ($\alpha = 0$). The white dashed lines indicate the positions of the electronic coordinate at the origin $z = 0$ a.u. and the equilibrium internuclear distance $z = \pm 1.3$ a.u., respectively. The other laser parameters are the same as those in Fig. 1(a1).

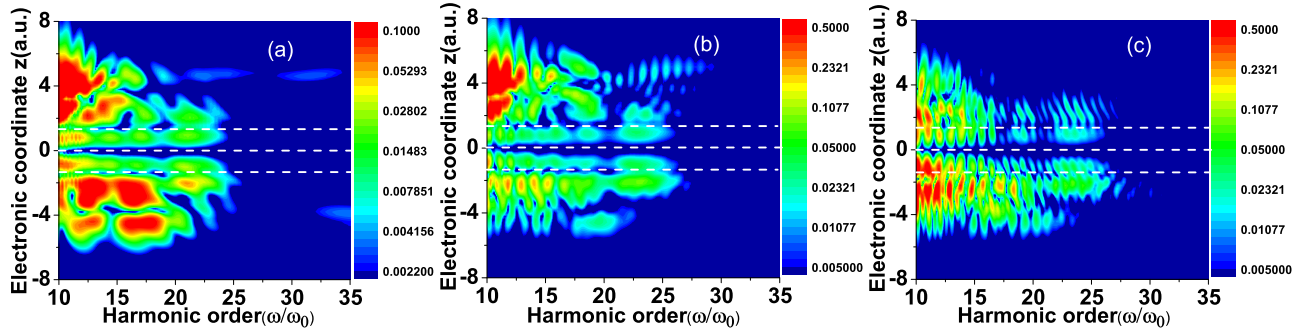


FIG. 3. (Color online) Spatial distribution of the HHG spectra as a function of electronic coordinate and harmonic order for different FWHMs (a) $\tau = 3$ fs, (b) $\tau = 5$ fs, and (c) $\tau = 7$ fs in a Gaussian laser pulse with a static field ($\alpha = 0.4$). The other laser parameters are the same as those in Fig. 1(b1). The white dashed lines indicate the positions of the electronic coordinate at the origin $z = 0$ a.u. and the equilibrium internuclear distance $z = \pm 1.3$ a.u., respectively.

the equilibrium internuclear distance $z = \pm 1.3$ a.u. The electron localization is most likely to be removed at the equilibrium internuclear distance, which is illustrated experimentally [37]. The total energy of the molecule is the lowest at the equilibrium internuclear distance, which presents the most stable state of the H_2^+ molecule. From Fig. 1(a3) we know that the electron moves farther in the process of the recombination with the nucleus along the positive- z direction than that with the nucleus along the negative- z direction (in our coordinate system). It should be mentioned that the longer the electron accelerates, the higher the harmonic order is. Thus, the cutoff of HHG is larger when the electron recombines with the nucleus along the positive- z direction. At the same time, from Fig. 1(a1) we know that the ionization probability increases after its negative peak P_1 , but it is enhanced much higher after the positive peak P_2 . Thus, the harmonic intensity is more enhanced in the process of recombination with the nucleus along the negative- z direction than that with the nucleus along the positive- z direction (in our coordinate system), which is in accord with the spatial distribution in HHG as shown in Fig. 2(b).

Figure 3 shows the spatial distribution of the HHG spectra as a function of the electronic coordinate and harmonic order for different FWHMs in the Gaussian laser pulse with a static field ($\alpha = 0.4$). The intensity of the harmonics for each coordinate on the vertical axis is related to the probability of electronic recombination with the nucleus [25]. As shown in Fig. 3(a), the contribution to HHG mainly comes from the electronic coordinates $z = -6$ to 6 a.u. and the contribution from the nucleus along the negative- z direction (in our coordinate system) is higher for $\tau = 3$ fs. In addition, we can see that the harmonic intensity is predominant at two regions: the electronic coordinates $z = -3$ to -2 a.u. and around $z = 4$ a.u.; thus the probability of the recombination of the electron with the nucleus in these coordinates is larger. Figures 3(b) and 3(c) show the spatial distribution of the HHG spectra with FWHMs of 5 and 7 fs, respectively. It is also indicated that there is little contribution to the HHG around the origin $z = 0$ a.u. and equilibrium internuclear positions $z = \pm 1.3$ a.u. Thus we can draw the conclusion that this characteristic is attributed to the molecular structure and is irrelevant to laser parameters.

Figure 4 presents the time evolution of the nuclear probability distribution $P_R(R, t)$ to further illustrate the spatial distribution of the harmonic generation. Figure 4 shows

that the internuclear distance is around the equilibrium internuclear distance $R = 2.6$ a.u. at the beginning of the interaction between the laser pulse and the molecule (before $t = -0.23$ o.c.). When the laser reaches its maximum peak P_1' [as indicated in Fig. 1(b1)], the electron begins to ionize. Meanwhile, the internuclear distance becomes larger due to the Coulomb repulsion between the two nuclei and the maximum value is about 3.0 a.u., which provide strong evidence of our assumption of the recombination range in Fig. 1(b2). Thus, the electronic coordinate $|z|$ is greater than 1.3 a.u. when the electron recombines with the nucleus, which agrees with the harmonic intensity being higher when the electronic coordinate $|z|$ is greater than 1.3 a.u., as shown in Fig. 3(a). After the recombination process, the internuclear distance returns to its equilibrium distance to keep stable.

To clarify the spatial distribution of the HHG spectra illustrated in Fig. 3(a), we illustrate the probability density distributions of the coupled electron nuclear wave packet for the time evolution from $t = -1.0$ to 0.75 o.c. in Fig. 5. We can see that the electron is mainly distributed around the electronic

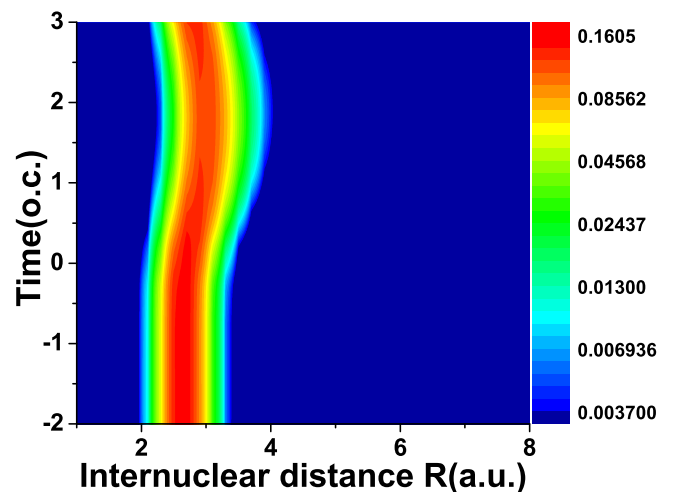


FIG. 4. (Color online) Contour plot of the time evolution of the nuclear probability distribution $P_R(R, t)$ calculated from the 1D non-Born-Oppenheimer approximation TDSE for the H_2^+ molecule. The other laser parameters are the same as those in Fig. 1(b1).

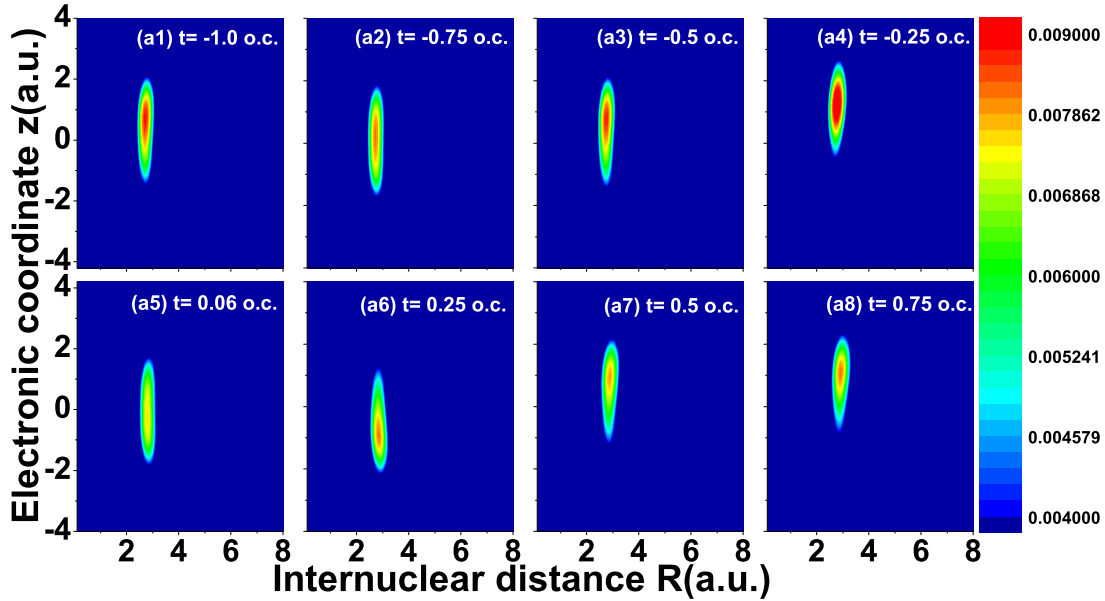


FIG. 5. (Color online) Probability density distributions of the coupled electron nuclear wave packet for the time evolution from $t = -1.0$ to 0.75 o.c. with each time interval 0.25 o.c. The other laser parameters are the same as those in Fig. 1(b1).

coordinate $z > 0$ at $t = -1.0$ o.c. and then is distributed evenly around the region of the electronic coordinate $z = 0$ at $t = -0.75$ o.c. As the electric field is a negative value at this time, the electron is more likely along the positive- z direction and cannot recombine with the nucleus as shown in Fig. 1(b3). The ionized electron (around $t = 0.06$ o.c.) is along the negative- z direction because the electric field is a positive value at this time. When the laser reverses, the electron can return and has a larger probability of recombining with the nucleus along the negative- z direction (in our coordinate system), which is in agreement with the analysis in Fig. 1(b3). This phenomenon is also mentioned in Ref. [36]. With the time evolution, the electron is mainly distributed in the region along the positive- z direction since the electric field is always a negative value.

The ionization probability shown in Fig. 1(b1) indicates that the electron is ionized again around $t = 0.06$ o.c. The emission time for the short trajectories is around 0.75 o.c., as shown in Fig. 1(b2), and this is the process that mainly contributes to the high-order-harmonic generation. To get a deeper insight into the process of ionization and recombination, the total energy [9] of the Coulomb potential and laser field potential at $t = 0.06$ and 0.75 o.c. are shown in Figs. 6(a) and 6(b), respectively. The solid arrow in Fig. 6(a) shows the ionization process and the solid arrows in Fig. 6(b) show the recombination process. According to the probability density distributions of the electronic wave packet as shown in Fig. 1(b3), we can give the electronic positions in the region of the negative- z direction at both $t = 0.06$ and 0.75 o.c. (the electron is represented by the red dot in Fig. 6). The electron being ionized from the nucleus along the negative- z direction and recombined with the nucleus along the positive- or negative- z direction (in our coordinate system) is considered. Figure 6(a) shows that the left potential well is depressed, the right potential well is increased, and the potential barrier is formed at time $t = 0.06$ o.c. The electron located around the left potential

well can be ionized over the potential barrier. After that the electron is accelerated in the laser field. When the laser field changes its direction, the electron recombines with the nucleus along the positive- or negative- z direction. It is easier for the electron to recombine with the nucleus along the negative- z direction (in our coordinate system) for our one-dimensional model due to the fact that the electron is close to the left potential well at $t = 0.75$ o.c. In this case the electron tends to recombine with the nucleus along the negative- z direction (in our coordinate system), which is in agreement with the above analysis.

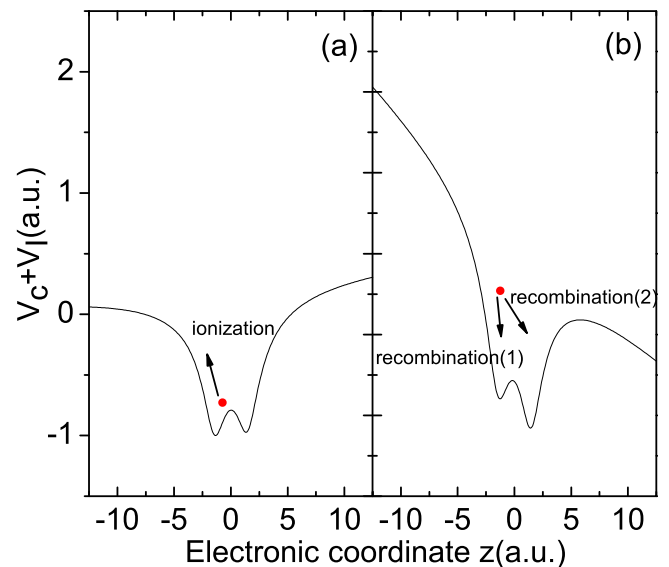


FIG. 6. (Color online) Combined energy of the Coulomb potential and laser field potential at time (a) $t = 0.06$ o.c. and (b) $t = 0.75$ o.c. The red dot represents the electron. The other laser parameters are the same as those in Fig. 1(b1).

IV. CONCLUSION

In summary, we have numerically solved the 1D TDSE within the non-Born-Oppenheimer approximation to investigate the spatial distribution in HHG in the H_2^+ molecule via the combination of a linearly polarized laser field with a Gaussian envelope and a static laser field. The results show that if the electric field reaches its negative peak, the electron is ionized along the positive- z direction. When the laser reverses, the electron slows down until it is pulled back and the contribution to the HHG mainly comes from the recombination of the electron with the nucleus along the positive- z direction. Meanwhile, if the electric field reaches its positive peak, the electron is ionized along the negative- z direction. When the laser reverses, the electron slows down until it is pulled back and the contribution to the HHG mainly comes from the recombination of the electron with the nucleus along the negative- z direction. The underlying physical mechanism can be well understood by the three-step model and the time-dependent

electron nuclear wave packet. We illustrate that there is little possibility of recombination of the electron with the nuclei around the origin $z = 0$ a.u. and equilibrium internuclear positions $z = \pm 1.3$ a.u. from the spatial distribution of the HHG spectra. We also demonstrate that this characteristic is attributed to the molecular structure. The harmonic intensity is higher when the absolute value of the electronic coordinate is greater than 1.3 a.u., which is illustrated by the time evolution of the nuclear probability distribution.

ACKNOWLEDGMENTS

The authors sincerely thank Professor Keli Han and Dr. Ruifeng Lu for providing us with the LZHDICP code. This work was supported by the National Natural Science Foundation of China (Grants No. 11104108, No. 11271158, and No. 11174108).

-
- [1] P. M. Paul, E. S. Toma, P. Breger, G. Mullot, F. Augé, Ph. Balcou, H. G. Muller, and P. Agostini, *Science* **292**, 1689 (2001).
 - [2] P. B. Corkum and F. Krausz, *Nat. Phys.* **3**, 381 (2007).
 - [3] C. Winterfeldt, C. Spielmann, and G. Gerber, *Rev. Mod. Phys.* **80**, 117 (2008).
 - [4] R. Kienberger, M. Hentschel, M. Uiberacker, Ch. Spielmann, M. Kitzler, A. Scrinzi, M. Wieland, Th. Westerwalbesloh, U. Kleineberg, U. Heinzmann, M. Drescher, and F. Krausz, *Science* **297**, 1144 (2002).
 - [5] S. Baker, J. S. Robinson, C. A. Haworth, H. Teng, R. A. Smith, C. C. Chirilă, M. Lein, J. W. G. Tisch, and J. P. Marangos, *Science* **312**, 424 (2006).
 - [6] P. B. Corkum, *Phys. Rev. Lett.* **71**, 1994 (1993).
 - [7] K. J. Schafer, B. Yang, L. F. DiMauro, and K. C. Kulander, *Phys. Rev. Lett.* **70**, 1599 (1993).
 - [8] M. Lewenstein, Ph. Balcou, M. Yu. Ivanov, A. L'Huillier, and P. B. Corkum, *Phys. Rev. A* **49**, 2117 (1994).
 - [9] X. Y. Miao and H. N. Du, *Phys. Rev. A* **87**, 053403 (2013).
 - [10] B. K. McFarland, J. P. Farrell, P. H. Bucksbaum, and M. Gühr, *Phys. Rev. A* **80**, 033412 (2009).
 - [11] O. Smirnova, Y. Mairesse, S. Patchkovskii, N. Dudovich, D. Villeneuve, P. Corkum, and M. Y. Ivanov, *Nature (London)* **460**, 972 (2009).
 - [12] Y. Pan, S. F. Zhao, and X. X. Zhou, *Phys. Rev. A* **87**, 035805 (2013).
 - [13] J. Guo, X. L. Ge, H. Zhong, X. Zhao, M. Zhang, Y. Jiang, and X. S. Liu, *Phys. Rev. A* **90**, 053410 (2014).
 - [14] T. Zuo and A. D. Bandrauk, *Phys. Rev. A* **52**, R2511(R) (1995).
 - [15] T. Seideman, M. Yu. Ivanov, and P. B. Corkum, *Phys. Rev. Lett.* **75**, 2819 (1995).
 - [16] G. Camiolo, G. Castiglia, P. P. Corso, E. Fiordilino, and J. P. Marangos, *Phys. Rev. A* **79**, 063401 (2009).
 - [17] X. Guan, K. Bartschat, B. I. Schneider, and L. Koesterke, *Phys. Rev. A* **88**, 043402 (2013).
 - [18] K. Doblhoff-Dier, K. I. Dimitriou, A. Staudte, and S. Gräfe, *Phys. Rev. A* **88**, 033411 (2013).
 - [19] K. J. Yuan and A. D. Bandrauk, *Phys. Rev. A* **83**, 063422 (2011).
 - [20] M. Lein, N. Hay, R. Velotta, J. P. Marangos, and P. L. Knight, *Phys. Rev. Lett.* **88**, 183903 (2002).
 - [21] X. B. Bian and A. D. Bandrauk, *Phys. Rev. Lett.* **105**, 093903 (2010).
 - [22] X. B. Bian and A. D. Bandrauk, *Phys. Rev. A* **83**, 023414 (2011).
 - [23] S. Chelkowski, C. Foisys, and A. D. Bandrauk, *Phys. Rev. A* **57**, 1176 (1998).
 - [24] A. D. Bandrauk, S. Chelkowski, and H. Lu, *J. Phys. B* **42**, 075602 (2009).
 - [25] X. L. Ge, T. Wang, J. Guo, and X. S. Liu, *Phys. Rev. A* **89**, 023424 (2014).
 - [26] X. Y. Miao and C. P. Zhang, *Laser Phys. Lett.* **11**, 115301 (2014).
 - [27] O. Sharafeddin and J. Z. H. Zhang, *Chem. Phys. Lett.* **204**, 190 (1993).
 - [28] C. J. Joachain, N. J. Kylstra, and R. M. Potvliege, *Atoms in Intense Laser Fields* (Cambridge University Press, Cambridge, 2012), Chap. 2.
 - [29] M. D. Feit and J. A. Fleck, Jr., *J. Chem. Phys.* **78**, 301 (1983).
 - [30] R. F. Lu, H. X. He, Y. H. Guo, and K. L. Han, *J. Phys. B* **42**, 225601 (2009).
 - [31] R. F. Lu, P. Y. Zhang, and K. L. Han, *Phys. Rev. E* **77**, 066701 (2008).
 - [32] J. Hu, K. L. Han, and G. Z. He, *Phys. Rev. Lett.* **95**, 123001 (2005).
 - [33] B. Feuerstein and U. Thumm, *J. Phys. B* **36**, 707 (2003).
 - [34] K. Burnett, V. C. Reed, J. Cooper, and P. L. Knight, *Phys. Rev. A* **45**, 3347 (1992).
 - [35] J. Wang, G. Chen, F. M. Guo, S. Y. Li, J. G. Chen, and Y. J. Yang, *Chinese Phys. B* **22**, 033203 (2013).
 - [36] Y. N. Pei and X. Y. Miao, *Chinese Phys. Lett.* **31**, 104202 (2014).
 - [37] X. Gong, Q. Song, Q. Ji, H. Pan, J. Ding, J. Wu, and H. Zeng, *Phys. Rev. Lett.* **112**, 243001 (2014).